

# Design and Simulation of an ABS Control Scheme for a Formula Student Prototype

João Pedro Ferro  
joaoferro@tecnico.ulisboa.pt

Instituto Superior Técnico, Lisboa, Portugal

May 2014

## Abstract

This thesis addresses the design of an anti-lock braking system (ABS) seeking the implementation on a *Formula Student* racing prototype. The proposed scheme utilizes a cascade control architecture: a PID-type fuzzy controller with a Takagi-Sugeno-Kang fuzzy inference system is designed for wheel slip control in the outer loop, whilst a brake pressure PD controller is adopted in the inner loop. A wheel slip estimation solution, resorted to a complementary filter, is also developed. The performance of the ABS is assessed with a full vehicle model, sustained by vehicle dynamic principles. The model is integrated with brakeline dynamics and a tire friction model based on reliable experimental data. Straight line brake simulations are performed and results are evaluated in terms of braking efficiency and control robustness, under different and variable conditions. A complete lap within a typical *Formula Student* circuit is also simulated with and without the use of ABS. **Keywords:** anti-lock braking system (ABS), *Formula Student*, fuzzy controller, PID controller, wheel slip estimation, vehicle model, tyre model

## 1. Introduction

The ABS is an active safety system present in most of passenger cars and trucks. It prevents wheel lock-up and minimizes braking distance, while ensuring the steering stability of the vehicle under hard braking. From a typical tire friction curve, depicted in Fig. 1, this is accomplished by controlling longitudinal wheel slip  $S_X$  (Eq. 1) within a desired range where peak longitudinal tire force is attained while maintaining adequate lateral force.

$$S_X = \frac{\omega_W R_L - v_X}{v_X} \quad (1)$$

where  $\omega_W$  is the wheel-spin velocity,  $v_X$  is the longitudinal vehicle velocity, and  $R_L$  is the tire loaded radius.

As the optimum value of  $S_X$  do not coincide for both tire longitudinal and lateral forces, respectively  $F_{XT}$  and  $F_{YT}$ , a compromise is frequently necessary near the absolute value of 0.2. Hence, the ABS design is inherently related with the problem of wheel slip control. In practical terms, since vehicle speed  $v_X$  cannot be directly controlled, wheel slip control is executed by controlling wheel angular velocity  $\omega_W$  alone, which in turn is accomplished by manipulating the brake pressure on the wheel caliper  $p_{cal}$ .

### 1.1. Background

Beyond the inestimable contribution to road safety, ABS may also be used in racecars as a driving-aid system for enhanced braking performance and reduced tire wear. Although forbidden in most high-end racing disciplines like Formula 1, driving-aids like ABS are allowed in Formula Student (FS) and teams may benefit from its implementation. FS is a motorsport and engineering competition between university teams across the globe, where students are challenged to design and build a single-seat racing car. At *Instituto Superior Técnico*, *Projecto FST* team has recently built its fifth and most innovative prototype FST 05e. The availability of new development tools (sensors on the car, computer car model) allied with the constant seek for best performance possible has cleared the path for the implementation of an ABS for the first time. The purpose of this work is thus to design and model an effective and reliable solution for the ABS control problem that can also be simple and inexpensive to implement on a FS prototype.

### 1.2. Literature Review

Several approaches to the ABS control problem have been developed and documented in the literature. Conventional threshold is the simplest and

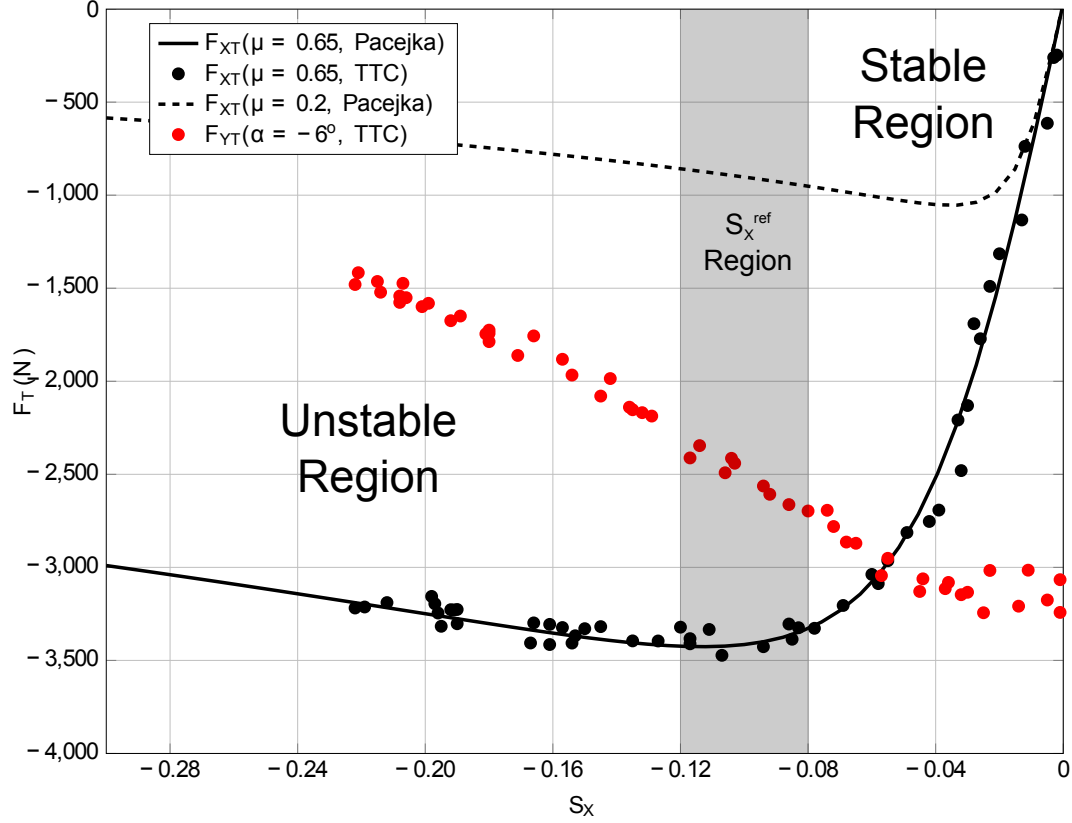


Figure 1: ABS action zones.

primary technique used for wheel slip [1, 2]. However, the pronounced nonlinearity and uncertainty of the system to be controlled, mainly due to the complex friction between tire and road interaction, has demanded for other adaptive and robust control methods. Some of the most relevant and efficient approaches were reviewed, namely the hybridization of conventional PID [3, 4], sliding-mode control [5, 6, 7, 8], fuzzy control [9, 10] and neuro-fuzzy control [11, 12, 13].

## 2. Vehicle and Tire Model

For the ABS design process and further simulation, a vehicle model with 14 DOFs was built upon the mechanical, physical and aerodynamic principles of vehicle dynamics [14, 15]. For an ABS applications, dynamics under braking and tire-road interaction are the most important aspects to consider. The developed full vehicle model is composed by five interdependent sub-models, as represented in Fig. 2.

**Horizontal dynamics** is a 3-degrees of freedom (DOFs) model of vehicle position ( $x_E$  and  $y_E$ ) and orientation (yaw angle  $\psi$ ) in the inertial

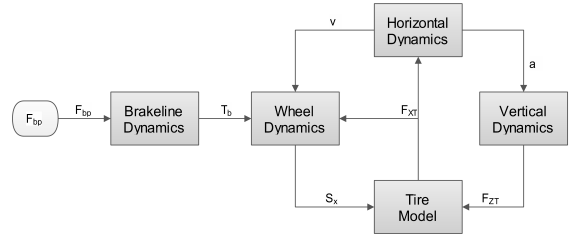


Figure 2: Vehicle dynamics overview.

reference plane. It resembles the kinematics of the vehicle's CG as a result of the applied tire forces and moments from the *Tire Model*.

**Vertical dynamics** are modelled in 7-DOFs vibrational model of the vehicle subjected to load transfer (proportional to acceleration) and aerodynamic forces (proportional to velocity). This model allows the transient computation of the individual tire vertical loads, and the vertical displacements of the sprung mass  $z_s$ , unsprung masses  $z_{u,FL}$ ,  $z_{u,FR}$ ,  $z_{u,RL}$  and  $z_{u,RR}$ ,

roll  $\phi$ , and pitch  $\theta$ .

**Brakeline Dynamics** model the hydraulic braking system, which for an ABS-equipped vehicle also include a hydraulic modulator. Given an external input of pedal brake force, it outputs the brake torque that is sent to the *Wheel Dynamics*.

**Wheel dynamics** applies the brake torque from *Brakeline Dynamics* and the current tire longitudinal force from the *Tire Model* and calculates the resulting wheel angular acceleration. The real-time calculation of longitudinal slip ratio  $S_X$  that is returned to the *Tire Model* is also part of the *Wheel Dynamics*.

**Tire model** is an empirical model of the complex friction dynamics between the tire and the pavement. It maps the tire forces and moments as a function of a set of input variables, namely the longitudinal slip ratio  $S_X$  and tire vertical load.

### 2.1. Tire Model

Tires are the primary source of the tractive, braking, and cornering forces/torques that provide the handling and control of a car. An accurate tire friction model is, thus, of absolute importance for ABS design. Three types of tire models were designed and compared:

**Pacejka Model** The most widely used semi-empirical tire friction model. It is given by the so-called parametric Magic Formula (MF) (Eq. 2) [16], whose coefficients support a set parametric functions dependent on the rolling conditions (e.g., tire vertical load).

$$y = D \sin[C \arctan\{Bx - E(Bx - \arctan Bx)\}] \quad (2)$$

$$Y(X) = y(x) + S_V \quad (3)$$

$$x = X + S_H \quad (4)$$

**Burkhardt Model** Is a simpler parametric model given by the following velocity-dependent parametric expression [6, 17]:

$$F(x) = [A(1 - e^{-Bx}) - Cx] e^{-Dxv} \quad (5)$$

**Neural Network Model** Is a versatile self-developed model that takes advantage of the effectiveness of artificial neural network (ANN) for nonlinear curve fitting.

The aforementioned models are used to fit reliable experimental data retrieved from the tests conducted at Calspan *Tire Research Facility* (TIRF).

For the parametric Pacejka and Burkhardt models, the least squares method approach (Eq. 6) is used to find the set of parameters  $\mathbf{p} = p_i$  that minimizes error to the experimental data. Neural Network model fitting is achieved by iterative network training.

$$\min_{\mathbf{p}} \sum_i r_i^2 = \sum_i (F(\mathbf{p}, x_i) - y_i)^2 \quad (6)$$

Fitting results, exhibited in Fig. 3 for the Pacejka model, indicate that this provided accurate longitudinal tire force  $F_{XT}$  mapping for a wider range of possible  $S_X$ , including the wheel lock-up case where  $S_X$  reaches -1. For the other two models, though a good fit is achieved within the limits of experimental data availability, the accurateness of the model is compromised for extrapolation beyond this limit.

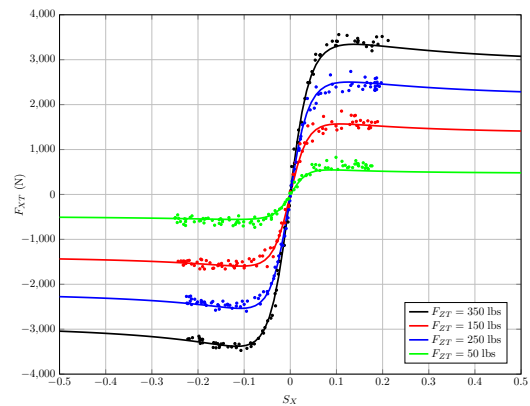


Figure 3: Pacejka Model vs. TTC Data for  $F_{ZT} = \{150, 250, 350\}$  lbs.

## 3. ABS Design

### 3.1. Proposed Approach

The cascade control architecture with two feedback loops shown in Fig. 4 is proposed for the ABS problem. On the outer loop, a PID-fuzzy wheel slip controller compares the actual wheel slip  $S_X$  with a given reference and outputs a reference pressure  $p_b^{ref}$  accordingly. This reference pressure is then sent to a conventional PD brake pressure controller, in the inner loop, which in turn sends a command signal  $u$  to the hydraulic modulator (actuator) so the reference pressure is matched.

This cascade arrangement means that the pressure controller deals only with the fast brakeline dynamics, allowing the wheel slip controller to exclusively deal with the slower remaining vehicle dynamics, enhancing the combined performance of the controllers. Moreover, the combination of the well-known PID principles with the intuitive theory and

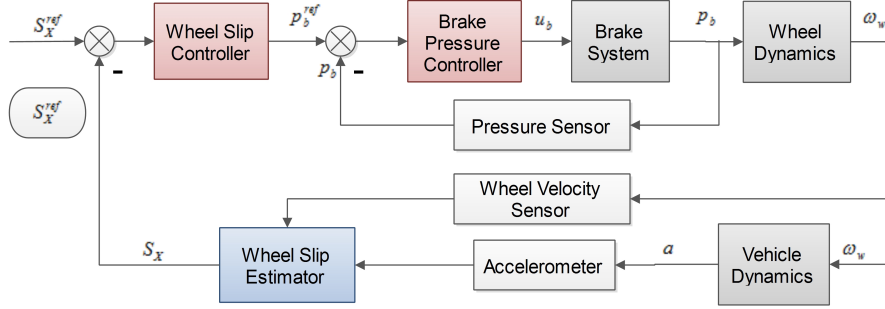


Figure 4: Proposed control structure.

computational efficiency of fuzzy inference systems (FISs) provides a simple design and implementation solution.

### 3.2. Brake Pressure Controller

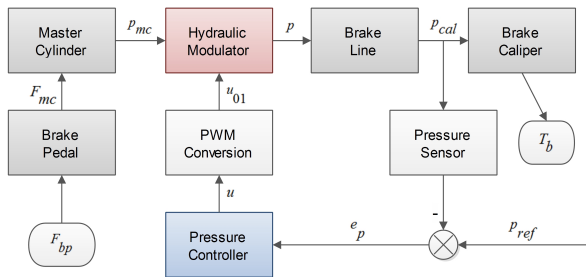


Figure 5: Schematic of brakeline dynamics and pressure controller.

Since the hydraulic modulator (actuator) only receives binary signals for the inlet and outlet valves, the analog control signal  $u$  outputted by the pressure controller has to be previously converted in two on-off signals  $u_{in}$  and  $u_{out}$  (Fig. 5). The pulse-width modulation (PWM) technique is used for the purpose. Two sawtooth wave signals with frequency  $f_c$  are generated, one ranging between  $[0\ 1]$  for the inlet valve, and  $[-1\ 0]$  for the outlet signal. Figure 6 depicts the conversion method for an example control signal.

Due to the resulting dynamic characteristics of the inner loop plant, i.e., brakeline and hydraulic modulator system, the regular Ziegler-Nichols methods for open and closed loop cannot be applied. Therefore, the model of the PWM conversion and the plant is approximated by the linearisable function (assuming  $p_{mc} = \infty$ ):

$$\frac{dp}{dt} = a \cdot \tanh(b \cdot u + h) + v \quad (7)$$

PD gains are then tuned, using Matlab's *PID Tuning* tool with the approximate system, in order to achieve the desired fast dynamics, near the actuator limit, without overshoot, which could let the

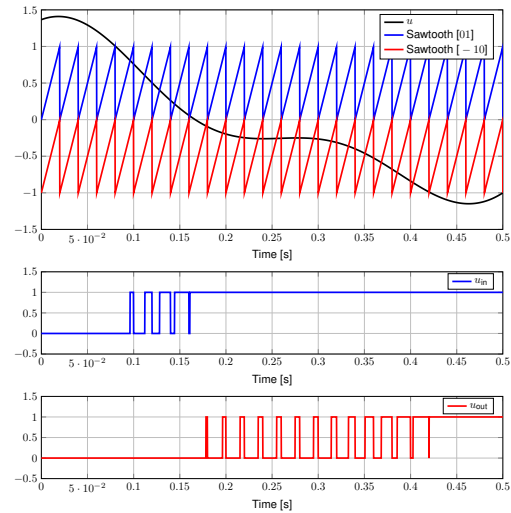


Figure 6: PWM implementation with  $f_c = 50$  Hz.

wheel slip to the unstable region of the tire friction curve. Integral effect is already inherent to the system. Figure 7 displays the controlled step response of the original system and shows that it was possible to eliminate the overshoot whilst maintaining a very fast response.

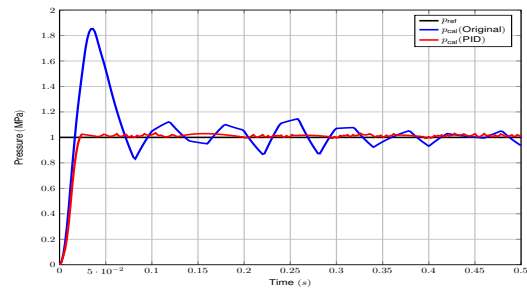


Figure 7: Step response with PD controller for  $p_{cal}$ .

### 3.3. Wheel Slip Controller

The proposed PID-fuzzy controller resorts on a zero-order Takagi-Sugeno-Kang (TSK) FIS with two input variables for the slip error  $e_{S_X}$  and its variation  $\Delta e_{S_X}$ . The output variable is selected to be the reference pressure variation  $\Delta p_b^{ref}$ , since the optimal pressure varies with velocity, and also to ensure that the designed controller will be more robust against parameter uncertainty and disturbances that, otherwise, would require an adaptive controller.

As depicted in Fig. 8 before entering the FIS, both input variables are multiplied by the gains  $K_e$  and  $K_{\Delta e}$ , which equivalent to the proportional and derivative gains of a PID controller. On the other side, the output of the FIS is multiplied by the gain  $K_{\Delta p}$  before integration.

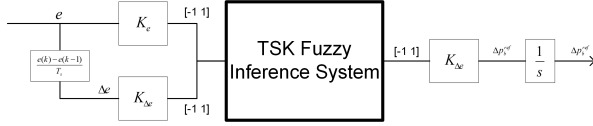


Figure 8: PID-type fuzzy controller scheme [4].

For the TSK fuzzy inference system, a set of fuzzy rules is defined in the form

$$R_r : \text{If } e_{S_X} \text{ is } A_i \text{ and } \Delta e_{S_X} \text{ is } B_j \\ \text{then } \Delta p_b^{ref} \text{ is } C_k \quad (8)$$

where  $A_i$  and  $B_j$  are the input fuzzy sets, and  $C_k$  is the output constant, as defined in Tab. 1. Rules are established according to the correspondance in Tab. 2.

$y_k$	Fuzzy Set	$C_k$
1	Decrease-fast ( $D_f$ )	-1
2	Decrease-slow ( $D_s$ )	-0.5
3	Hold ( $H$ )	0
4	Increase-slow ( $I_s$ )	0.5
5	Increase-fast ( $I_f$ )	1

Table 1: TSK consequent function parameters for output  $\Delta p_b^{ref}$ .

$A_i \backslash B_j$	Decreasing	Steady	Increasing
Negative	$I_f$	$I_s$	$H$
Zero	$I_s$	$H$	$D_s$
Positive	$H$	$D_s$	$D_f$

Table 2: Fuzzy rules for wheel slip controller.

Similar membership functions (MFs) for each of the fuzzy input sets are defined by Gaussian curves

(Eq. 9) and evenly distributed within the normalized interval  $[-1 1]$  (universe of discourse), as depicted in Fig. 9. Doing so ensures that the controller dynamics are easily adjusted solely by tuning the PID gains outside the FIS.

$$mf(x) = \text{Gaussian}(x; c, \sigma) = e^{-\frac{(x-c)^2}{2\sigma^2}} \quad (9)$$

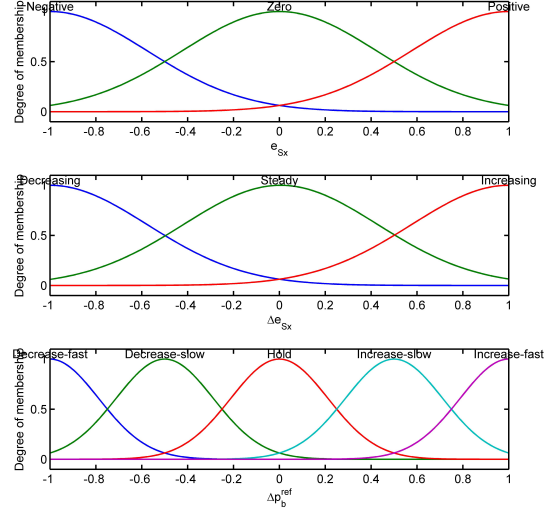


Figure 9: Membership functions of FIS.

The final output is computed as a weighted average of the output  $y_k$  of each rule:

$$\Delta p_b^{ref} = \frac{\sum_{ij} w_{ij} \cdot y_{ij}}{\sum_{ij} w_{ij}} \quad (10)$$

where the firing strength  $w_r$  of the rule is calculated using min as the AND (T-norm) operator [18]. The output surface of the designed FIS displayed in Fig. 10. In general, the reference pressure variation  $\Delta p_b^{ref}$  is more or less inversely proportional to the inputs, as in a PD controller. Slight variations of this linear relation, shown by the humps and valleys on the surface plot, ensure the adaptation of the controller on whether the system is evolving near/far from the reference slip or within/towards the stable/unstable region of the friction curve.

Input and output gains  $K_e$ ,  $K_{\Delta e}$  are tuned so the signal entering the FIS would range within the normalized interval  $[-1 1]$ . As for the output gain  $K_{\Delta p}$ , the value is chosen according to the actuator limits of pressure increase/decrease rate. Fine tuning is then performed until the desired controller response is achieved. Finally, different values for reference wheel slip  $S_X^{ref}$  near the peak longitudinal force are iteratively tested for minimum braking distance.

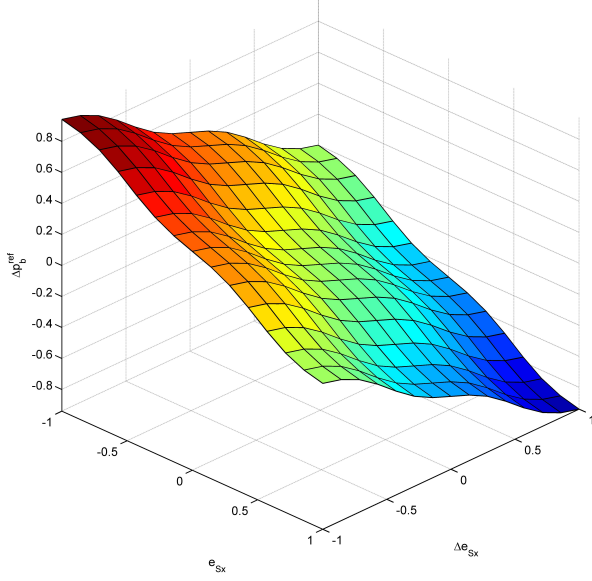


Figure 10: Output surfaces of FIS models for wheel slip controller.

### 3.4. Wheel Slip Estimator

Recalling Eq. 1, wheel slip computation depends on both wheel velocity  $\omega_W$ , available through direct, yet noisy measurements from the equipped wheel encoders, and vehicle inertial velocity  $v_X$ , which cannot be directly measured without impractical and expensive equipment [19]. Hence, the problem of estimating the longitudinal wheel slip  $S_X$  is crucial for an effective implementation of an ABS controller.

Additionally to the controllers, a wheel slip estimator is designed using a complementary filter, i.e., a Wiener filter equivalent to the stationary Kalman filter solution (Fig. 11). The estimation merges information provided by sensors over distinct, yet complementary frequency regions [20]. In this particular case, low frequency measurements provided by the mounted accelerometer are combined with high frequency data from the wheel speed encoders:

$$\hat{v}_S = K(\omega_m R_e - (\hat{v}_S + v_m)) \quad (11)$$

where

$$\omega_{W,m} \equiv \omega_m = \omega_W + w_\omega \quad (12)$$

$$v_{X,m} \equiv v_m = \int(a_X + w_a) \quad (13)$$

As depicted in Fig. 12, a good estimation is achieved despite the noisy measured data. Moreover, different choices of gain  $K$  translate in a compromise between fast convergence and steady-state smoothness. Higher values favor high frequency measurements from wheel encoders and thus a noisier response is attained.

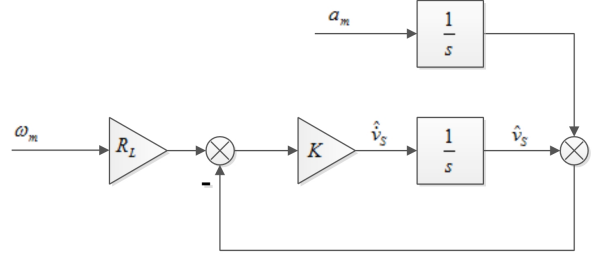


Figure 11: Block diagram of complementary filter.

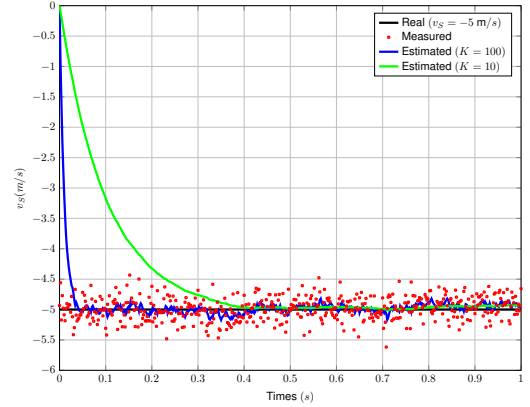


Figure 12: Slip velocity  $v_S$  estimation results with complementary filter.

The estimate longitudinal slip ratio is then calculated as:

$$\hat{S}_X = \frac{\hat{v}_S}{\int a_m} \quad (14)$$

### 3.5. ABS Triggers

To ensure the correct operation of the ABS, the following on and off thresholds are defined:

**Minimum brake pressure** Ensures that the ABS is on when, and only when the brake pedal is stepped. A threshold of 0.1 MPa for the caliper pressure  $p_{cal}$  is chosen.

**Wheel slip and wheel slip rate trigger** If wheel slip is beyond reference (unstable region) or decreasing at a high rate (towards lock-up), ABS should start the control cycle. Otherwise, normal brake applies. Trigger values are defined as  $S_X = -0.1$  and  $\Delta S_X = -2$ .

**Low velocity trigger** Since  $\lim_{v_X \rightarrow 0} S_X = \frac{0-0}{0}$ , a minimum velocity of 10 km/h is defined, below which the ABS is switched off to avoid increasingly bigger oscillations around the reference wheel slip that exceedingly degrade ABS

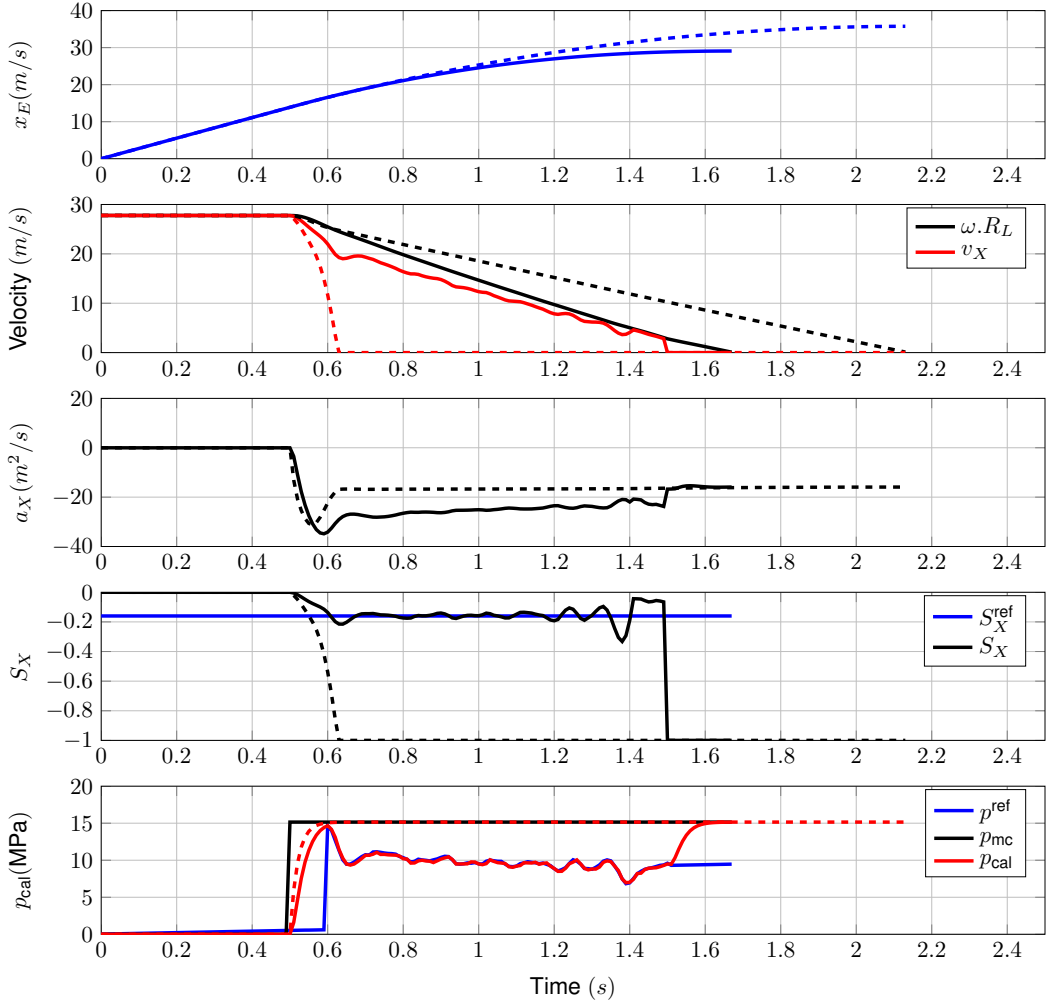


Figure 13: Comparative simulation results with (solid) and without (dashed) ABS.

efficiency and could even drive the system towards instability.

#### 4. Simulation Results

The performance of the proposed ABS control scheme is tested on the aforementioned full vehicle and tire model with a series of simulations on the Simulink environment. Data for the FST 05e prototype is taken from experimental measurements or CAD tools, and introduced in the model for an accurate simulation.

##### 4.1. Straight Line Hard Braking

The first set of simulations is performed for a simple hard braking manoeuvre: initially the vehicle travels at constant velocity  $v_X = 100$  km/h; at  $t = 0.5$  s, the *driver* steps hard on the pedal brake (so that  $T_b \gg F_{XT} \cdot R_L$ ) and keeps it until the vehicle stops.

With a constant road coefficient of friction  $\mu = 0.80$ , results over time with and without ABS are compared in Fig. 13. Up to  $t = 1$  s wheel tangential velocity  $\omega \cdot R_L$  equals the vehicle velocity, i.e., wheel is in free-rolling condition with  $S_X = 0$ . For the case without ABS (dashed line), when the *driver* starts braking the wheel rapidly decelerates, until it locks-up at  $S_X = -1$ . If the vehicle is equipped with the designed ABS controller, wheel velocity decreases until the reference slip  $S_X^{ref} = -0.16$  is matched and efficiently tracked.

Regarding the  $a_X$  plot, it is noticeable that for both cases a minimum acceleration is soon reached. As expected, this occurs when  $S_X = S_X^{ref}$ , i.e., when  $S_X$  crosses the optimal value for which peak longitudinal force is attained, as shown in Fig. 1. However, the ABS is able to keep this minimum thenceforth, thus resulting in a steeper velocity plot, and a smaller braking time and distance

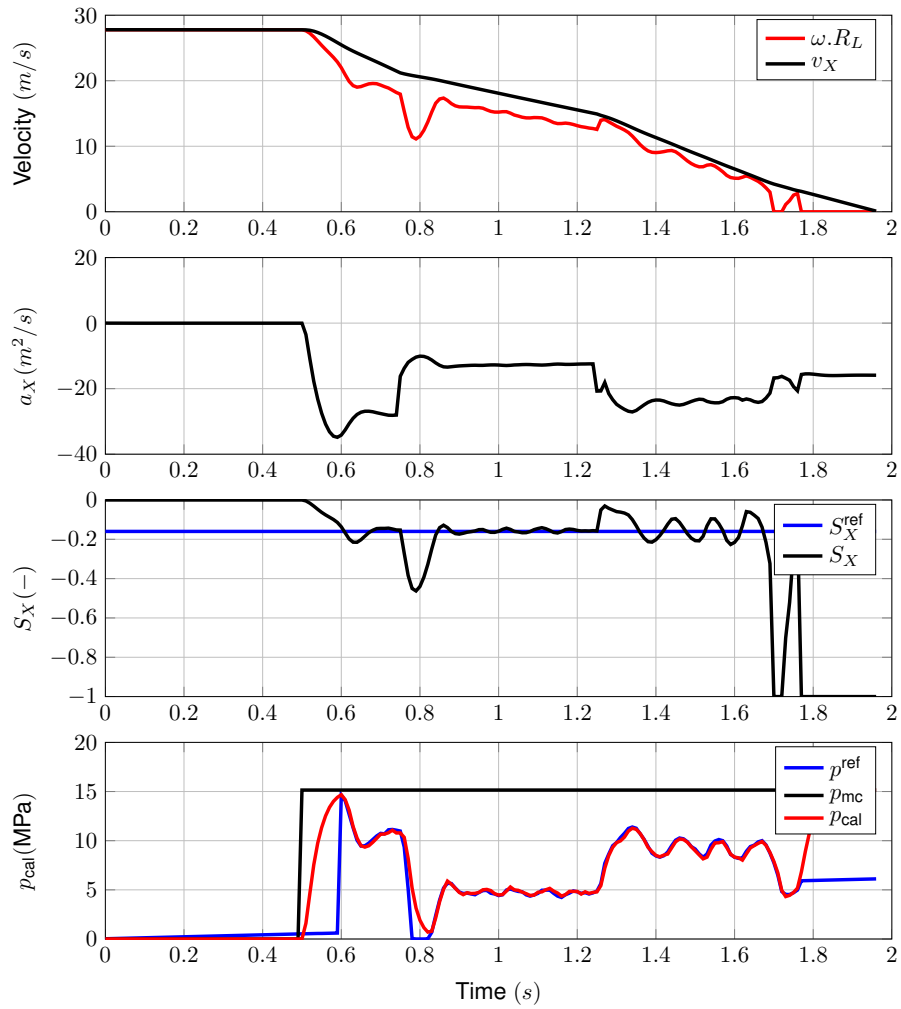


Figure 14: Simulation results with varying  $\mu$ .

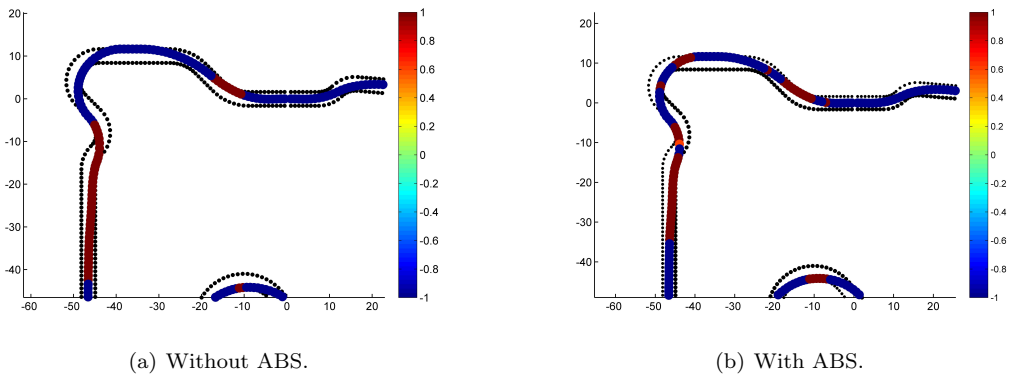


Figure 15: Brake plot over a typical FS lap.

(Tab. 3).

Observing the pressure plot for a braking without

ABS, pressure on the caliper quickly matches the pressure on the master cylinder (a certain dynamic can be noticed). On the other hand, the ABS managed to initially increase pressure at the maximum rate allowed by the actuator. The increase rate is then slowed to avoid overshoot when the wheel slip approaches the reference value.

	Distance (m)	Time (s)
Without ABS	21.87	1.63
With ABS	15.21	1.17
$\Delta$	-6.66	-0.46
$\% \Delta$	-30.5 %	-28.2 %

Table 3: Braking distance and time results with and without ABS.

#### 4.2. Varying Road $\mu$

To test the adaptivity of the designed ABS controller to real-time road-type changes, varying values for the road coefficient of friction  $\mu$  have been introduced as input parameter on the Pacejka tire model according to Eq. ??.

$$\begin{cases} \mu = 0.8 & \text{for } t < 0.75s \\ \mu = 0.5 & \text{for } 0.75 \leq t < 1.25s \\ \mu = 0.8 & \text{for } t \geq 1.25s \end{cases} \quad (15)$$

The resulting plot on figure 14 evidence a fast adaptation of the controller with varying coefficient of friction. At  $t = 0.75$  s, the wheel slip controller manages to compensate for the sudden decrease in the available tire force, which lead the wheel towards lock-up, by immediately diminishing the reference pressure. After a brief acceptable undershoot, reference pressure stabilizes and the reference wheel slip is restored. At  $t = 1.25$  s, the opposite phenomenon occurs and brake pressure can again be moderately increased to maximize tire force.

#### 4.3. Complete Lap

The absolute advantage of the ABS on a FS prototype is more evident across a complete lap in a typical FS circuit. As described in Sec. 1, the absence of an ABS may lead to wheel lock, i.e.,  $S_X = -1$ , for which no lateral force is developed by the tires and longitudinal force is suboptimal. To reproduce this effect, an optimal GG diagram of the FST 05e is narrowed in the pure braking and combined acceleration regions. Figures 15 display a sequence of curves made with and without ABS. In the former case, one can noticed that the driver is able to brake later and while cornering. At the end of the lap, results indicate a reduction of 4 s.

Without ABS	With ABS	$\Delta$	$\% \Delta$
52.17 s	48.31 s	3.86 s	7.4%

Table 4: Lap time results with and without ABS.

## 5. Conclusions

This paper reported the design and implementation of an ABS solution for a FS prototype. The control scheme resorts on a cascade control architecture containing PID-type fuzzy system for wheel slip regulation, a conventional PD controller for brake pressure reference tracking. The ABS is designed and tested in a 14-DOFs vehicle model integrated with a Pacejka tire friction model and wheel slip estimator.

A set of hard braking simulations evidence the effectiveness of the proposed approach on reducing the braking time and distance. Results exhibit a fast response and smooth tracking a reference wheel slip value. Furthermore, the robustness of the controller against sudden variations of the road coefficient of friction  $\mu$ , both high-to-low and low-to-high, was also successfully demonstrated. A final simulation within a complete lap around an typical FS circuit conclusively confirmed the competitive advantage of an ABS-equipped FS prototype.

### 5.1. Future work and research

As stated in Sec. 1, further implementation of the proposed controller is a concern. Having that mind during the modelling and design phases, special attention has already been given to some important practical issues: sampling time, PWM conversion and noise filtering were all considered. Hence, hardware-in-the-loop validations and hardware realization on a real FS prototype are the natural steps to follow.

Further research is also recommended on the issues of stability over asymmetric  $\mu$  surfaces, and control complementary of ABS and the equipped electric motor or an active suspension system.

## References

- [1] *Bosch Automotive Handbook*, Electronic ed., Robert Bosch GmbH, 2002.
- [2] K. Z. Rangelov, "Simulink model of a quarter-vehicle with an anti-lock braking system," Master's thesis, Eindhoven University of Technology, March 2004.
- [3] F. Jiang and Z. Gao, "An application of nonlinear PID control to a class of truck ABS problems," in *Proceedings of the 40th IEEE Conference on Decision and Control*, vol. 1, 2001, pp. 516–521 vol.1.

- [4] C.-K. Chen and M.-C. Shih, "PID-Type Fuzzy Control for Anti-Lock Brake Systems with Parameter Adaptation," *JSME International Journal Series C*, vol. 47, pp. 675–685, 2004.
- [5] E. Kayacan, Y. Oniz, and O. Kaynak, "A grey system modeling approach for sliding-mode control of antilock braking system," *IEEE Transactions on Industrial Electronics*, vol. 56, no. 8, pp. 3244–3252, Aug 2009.
- [6] A. Harifi, A. Aghagolzadeh, G. Alizadeh, and M. Sadeghi, "Designing a sliding mode controller for antilock brake system," in *The International Conference on Computer as a Tool (EUROCON)*, vol. 1, Nov 2005, pp. 258–261.
- [7] N. Patra and K. Datta, "Sliding mode controller for wheel-slip control of anti-lock braking system," in *IEEE International Conference on Advanced Communication Control and Computing Technologies (ICACCCT)*, Aug 2012, pp. 385–391.
- [8] Y. Tang, X. Zhang, D. Zhang, G. Zhao, and X. Guan, "Fractional order sliding mode controller design for antilock braking systems," *Neurocomputing*, vol. 111, no. 0, pp. 122 – 130, 2013.
- [9] A. Mirzaei, M. Moallem, B. Dehkordi, and B. Fahimi, "Design of an optimal fuzzy controller for antilock braking systems," *IEEE Transactions on Vehicular Technology*, vol. 55, no. 6, pp. 1725–1730, Nov 2006.
- [10] A. B. Sharkawy, "Genetic fuzzy self-tuning PID controllers for antilock braking systems," *Engineering Applications of Artificial Intelligence*, vol. 23, no. 7, pp. 1041 – 1052, 2010.
- [11] A. V. Topalov, Y. Oniz, E. Kayacan, and O. Kaynak, "Neuro-fuzzy control of antilock braking system using sliding mode incremental learning algorithm," *Neurocomputing*, vol. 74, no. 11, pp. 1883 – 1893, 2011.
- [12] N. Raesian, N. Khajepour, and M. Yaghoobi, "A new approach in anti-lock braking system (ABS) based on adaptive neuro-fuzzy self-tuning PID controller," in *2nd International Conference on Control, Instrumentation and Automation (ICCIA)*, Dec 2011, pp. 530–535.
- [13] W.-Y. Wang, M.-C. Chen, and S.-F. Su, "Hierarchical fuzzy-neural control of anti-lock braking system and active suspension in a vehicle," *Automatica*, vol. 48, no. 8, pp. 1698 – 1706, 2012.
- [14] R. N. Jazar, *Vehicle Dynamics: Theory and Application*. Springer, 2008.
- [15] T. D. Gillespie, *Fundamentals of Vehicle Dynamics*. SAE - Society of Automotive Engineers, Inc., 1992.
- [16] H. B. Pacejka, *Tyre and Vehicle Dynamics*, 3rd ed. Butterworth-Heinemann, 2012, ch. 4.
- [17] C. C. de Wit, P. Tsiotras, E. Velenis, M. Basset, and G. Gissinger, "Dynamic friction models for road/tire longitudinal interaction," *Vehicle System Dynamics*, vol. 39, no. 3, pp. 189–226, 2003.
- [18] J. Sousa and U. Kaymak, *Fuzzy Decision Making in Modeling and Control*, ser. World Scientific series in robotics and intelligent systems. World Scientific, 2002.
- [19] L. jun Wu, "Experimental study on vehicle speed estimation using accelerometer and wheel speed measurements," in *Second International Conference on Mechanic Automation and Control Engineering (MACE)*, 2011, pp. 294–297.
- [20] P. Oliveira, "Periodic and non-linear estimators with applications to the navigation of ocean vehicles," Ph.D. dissertation, UTL-Instituto Superior Tecnico, July 2002.